Ann. Geophys., 26, 2061–2067, 2008
www.ann-geophys.net/26/2061/2008/

Annales Geophysicae

The role of the vertical $E \times B$ drift for the formation of the longitudinal plasma density structure in the low-latitude F region

S.-J. Oh[1,*], H. Kil[2], W.-T. Kim[1], L. J. Paxton[2], and Y. H. Kim[3]

[1]Department of Physics and Astronomy, FPRD, Seoul National University, Seoul, Korea
[2]Applied Physics Laboratory, Johns Hopkins University, Laurel, MD, USA
[3]Department of Astronomy and Space Science, Chungnam National University, Daejeon, Korea
[*]now at: SELab, Seoul, Korea

Received: 24 July 2007 – Revised: 18 April 2008 – Accepted: 29 May 2008 – Published: 30 July 2008

Abstract. The formation of a longitudinally periodic plasma density structure in the low-latitude F region by the effect of vertical $\boldsymbol{E} \times \boldsymbol{B}$ drift was investigated by analyzing the ROCSAT-1 satellite data and conducting SAMI2 model simulations. The daytime equatorial ionosphere observed during the equinox in 1999–2002 from ROCSAT-1 showed the formation of wave number-4 structures in the plasma density and vertical plasma drift. The coincidence of the longitudes of the peak density with the longitudes of the peak upward drift velocity during the daytime supported the association of the longitudinal density structure with the vertical $\boldsymbol{E} \times \boldsymbol{B}$ drift. The reproduction capability of the observed wave-4 structure by the effect of vertical $\boldsymbol{E} \times \boldsymbol{B}$ drift was tested by conducting SAMI2 model simulations during the equinox under solar maximum condition. When the ROCSAT-1 vertical drift data were used, the SAMI2 model could reproduce the observed wave-4 density structure in the low-latitude F region. On the other hand, the SAMI2 model could not reproduce the observed wave-4 structure using the Scherliess and Fejer vertical $\boldsymbol{E} \times \boldsymbol{B}$ drift model. The observation and model simulation results demonstrated that the formation of the longitudinally periodic plasma density structure can be explained by the longitudinal variation of the daytime vertical $\boldsymbol{E} \times \boldsymbol{B}$ drift.

Keywords. Ionosphere (Electric fields and currents; Equatorial ionosphere; Modeling and forecasting)

1 Introduction

The formation of a longitudinally periodic plasma density structure in the low-latitude F region is now well known from extensive studies in recent years (Sagawa et al., 2005; Immel et al., 2006; Kil et al., 2007; Lin et al., 2007; Lühr et al., 2007; Scherliess et al., 2008). The observations of similar periodic structures in the daytime equatorial electrojet (England et al., 2006a; Mouël et al., 2006) and equatorial vertical ion velocity on the topside (Hartman and Heelis, 2007; Kil et al., 2007) supported the association of the longitudinal density structure with the daytime vertical drift of equatorial plasma. The diurnal non-migrating eastward-propagating tide with zonal wave number-3 (DE3 tide) was suggested as the driver of the longitudinal variation of the vertical $\boldsymbol{E} \times \boldsymbol{B}$ drift (England et al., 2006a, b; Immel et al., 2006) and Hagan et al. (2007) and showed the capability to produce the observed wave-4 density structure by the effect of the DE3 tide.

The observational, modeling, and theoretical studies in recent years have significantly advanced our understanding of the characteristics of the wave-like longitudinal density structure and its driving mechanism. These studies pointed to the zonal electric field or the vertical $\boldsymbol{E} \times \boldsymbol{B}$ drift of equatorial plasma as the source for this phenomenon. The formation of the equatorial ionization trough and equatorial ionization anomaly (EIA) by the effect of the vertical $\boldsymbol{E} \times \boldsymbol{B}$ drift is well known (e.g. Kelley, 1989). However, the formation of the periodic longitudinal density structure by the effect of the vertical $\boldsymbol{E} \times \boldsymbol{B}$ drift has not yet been verified, primarily due to the absence of a realistic model or observation that could represent the longitudinal variation of the vertical drift of equatorial plasma. The first Republic of China satellite (ROCSAT-1) provided temporally and spatially high-resolution vertical plasma drift data in the equatorial region and enabled us to test the capability to reproduce the observed longitudinal wave structure by the effect of the vertical $\boldsymbol{E} \times \boldsymbol{B}$ drift. To identify the role of the vertical $\boldsymbol{E} \times \boldsymbol{B}$ drift for the formation of the longitudinal density structure, we conducted the SAMI2 (Sami2 is Another Model of the Ionosphere (Huba et al., 2000)) model simulations using two different $\boldsymbol{E} \times \boldsymbol{B}$ drift inputs. One input vertical drift to the SAMI2 model was provided by the empirical $\boldsymbol{E} \times \boldsymbol{B}$ drift model developed

Correspondence to: S.-J. Oh
(oh@spweather.com)

Published by Copernicus Publications on behalf of the European Geosciences Union.

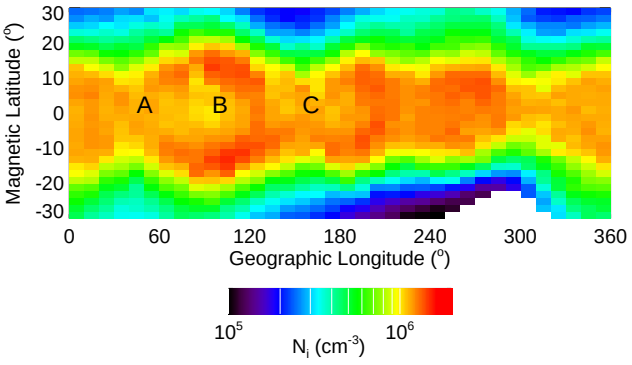

Fig. 1. The daytime longitudinal plasma density structure observed from ROCSAT-1. The mean density at each 10°×2° longitude-latitude bin was calculated using the ROCSAT-1 data at 12:00–14:00 LT during equinox (March, April, September, and October) in 1999–2002.

by Scherliess and Fejer (1999). The Scherliess and Fejer (SF) $E \times B$ drift model has represented the vertical drift of the equatorial plasma and is the default $E \times B$ drift in the SAMI2 model. The other input $E \times B$ drift to the SAMI2 model was provided by ROCSAT-1. We modified the SAMI2 model source program, so that the SF drift model is replaced by the ROCSAT-1 $E \times B$ drift. The ROCSAT-1 data sets for this study were produced using data during equinox in 1999–2002. The SAMI2 model simulations were conducted on 26 March 2002.

2 Longitudinal plasma density structure observed from ROCSAT-1

ROCSAT-1 had a low-inclination (35°) circular orbit at a mean altitude of 600 km. Its orbital period was 96 min. The total ion density was measured by the ion trap sensor and the cross-track ion drift velocity was measured by the ion drift meter (Su et al., 1999). It took about 25 days for a full coverage of the local time at a fixed longitude in low latitudes. The accuracy of the velocity measurements from the ion drift meter depends on the total ion density and the proportion of oxygen ions. The cross-track ion velocity can be determined accurately (error<10%) when the ion density is greater than 10^3 cm^{-3} and the percentage of the oxygen ion is greater than 85%. This condition is satisfied in most cases at an altitude of 600 km.

The temporal evolution of the wave-like longitudinal density structure in the ROCSAT-1 data showed the occurrence of the most pronounced wave structure just after noon (Kil et al., 2008). In Fig. 1, we present the mean plasma distribution at 12:00–14:00 LT obtained from ROCSAT-1. The mean density was calculated using the ROCSAT-1 data during equinox (March, April, September, and October) in 1999–2002 under the condition $K_p \leq 3^+$. The density map shows the occurrence of a wave number-4 structure in the low-latitude region with the density peaks near 10° E, 100° E, 200° E, and 280° E. The density peak is most pronounced near 100° E. The occurrence of the pronounced daytime density peak near 100° E was also identified by the observations of the Ocean Topography Experiment (TOPEX)/Poseidon mission (Scherliess et al., 2008). The figure shows the hemispheric symmetry of the wave-4 structure. Considering the minimal effect of the interhemispheric wind during equinox, the vertical $E \times B$ drift might play the dominant role for the formation of the longitudinal density structure.

3 SF vertical $E \times B$ drift model

Before we present the model simulation results, we briefly introduce the SF $E \times B$ drift model. The SF $E \times B$ drift model was developed using the Atmospheric Explorer-E (AE-E) satellite data from January 1977 to December 1979. The accuracy of the model drift in the Peruvian sector was improved by combining the AE-E data with the observations from the Jicamarca incoherent scattering radar during 1968–1992. The amplitudes of the model drift velocity were constrained using the curl-free nature of the zonal component of the electric field at the geomagnetic equator. The satellite and radar data sets were grouped into three seasons: June solstice (May–August), December solstice (November–February), and equinox (March–April, September–October). The solar activity was divided by two levels of F10.7 indices of 90 and 180. The longitude sectors were grouped based on the magnetic declination and the displacement of the magnetic equator from the geographic equator. The model $E \times B$ drift values can be obtained by cubic-B spline fitting of the AE-E and radar data with an input of local time, geographic longitude, day of the year, and F10.7 index.

Figure 2 shows the local time variations of the SF model $E \times B$ drift patterns at 45° E (dotted line), 95° E (solid line), and 155° E (dashed line) on 26 March 2002. The ROCSAT-1 data in Fig. 1 showed the occurrence of a density peak at 95° E and density minima at 45° E and 155° E. The vertical drift shows the typical upward drift on the dayside and downward drift at night, as was observed at Jicamarca (Fejer et al., 1999). The steep increase of the upward velocity around 18:00 LT is called the evening pre-reversal enhancement. The SF drift model does not show any notable longitudinal difference in the daytime vertical drift velocity at the three locations. We can identify slightly larger upward velocity at 155° E than at the other two longitudes before noon. As we will show in the following section, the SF model $E \times B$ drifts are largely different from the ROCSAT-1 observations.

4 SAMI2 model simulations

The SAMI2 (Huba et al., 2000) is an open source model and has been widely used to simulate plasma dynamics and the

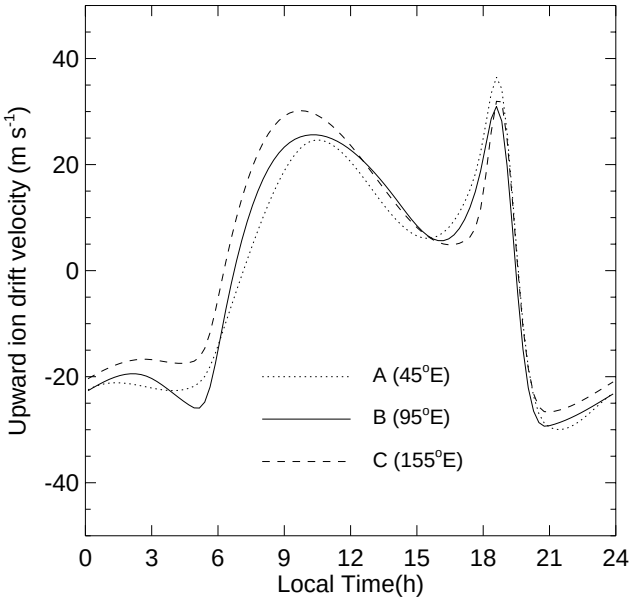

Fig. 2. The empirical SF model $\boldsymbol{E}\times\boldsymbol{B}$ drifts at 45° E (solid line), 95° E (dotted line), and 155° E (dashed line) on 26 March 2002.

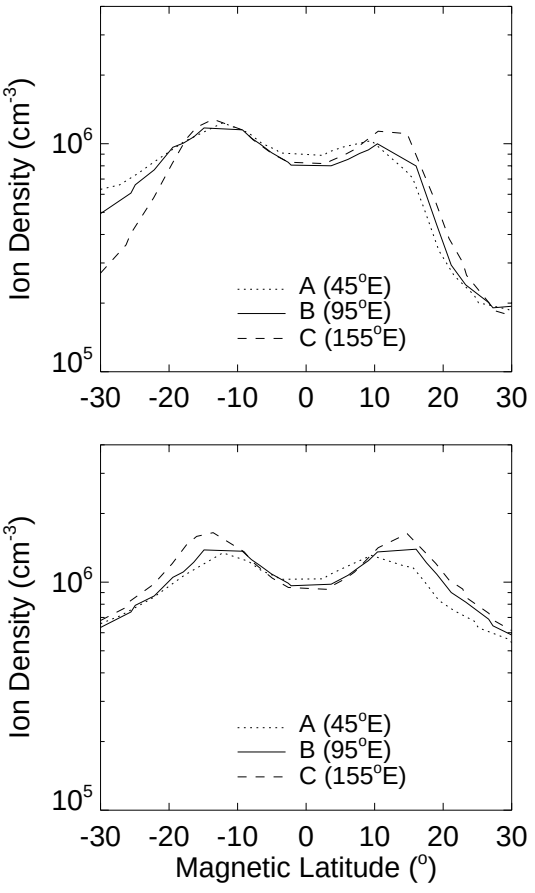

Fig. 3. SAMI2 model plasma density profiles at an altitude of 600 km at 12:00–14:00 LT on 26 March 2002. The top panel shows the density profiles obtained in the presence of the HWM wind. The bottom panel shows the density profiles obtained after the removal of the HWM wind.

chemical evolution of ion species in the low- and middle-latitude ionosphere. SAMI2 models the major ion species (H^+, He^+, N^+, O^+, $N_2{}^+$, NO^+, and $O_2{}^+$) along the Earth's geomagnetic field from hemisphere to hemisphere in the altitude range from 85 km to 20 000 km. The neutral atmosphere is specified using the empirical Mass Spectrometer Incoherent Scatter (MSIS) model (Hedin, 1991) and the Horizontal Wind Model (HWM) (Hedin et al., 1991). The input vertical $\boldsymbol{E}\times\boldsymbol{B}$ drift is specified using the empirical Scherliess and Fejer (1999) $\boldsymbol{E}\times\boldsymbol{B}$ drift model or it can be replaced by a simple sinusoidal curve. The model simulations were conducted on 26 March 2002 (AP index=11, F10.7 index=166, K_p=3$^-$) at 45° E, 95° E, and 155° E. We chose this day because the ROCSAT-1 observations in this study were made in equinox during a solar maximum period. The mean F10.7 index during equinox in 1999–2002 was 174. In our preliminary model simulations, the SAMI2 model produced higher plasma density than the ROCSAT-1 observations at the given conditions. To match the model plasma density to the ROCSAT-1 density at the EIA, we adjusted the multiplicative factor to oxygen ion to 0.75 (J. Huba, private communication, 2007).

The SAMI2 model simulations were conducted at the three longitude regions using the SF model $\boldsymbol{E}\times\boldsymbol{B}$ drifts shown in Fig. 2. The top panel in Fig. 3 shows the mean latitudinal density profiles at 12:00–14:00 LT at an altitude of 600 km obtained in the presence of HWM wind. The bottom panel shows the density profiles obtained after the removal of the HWM wind. The top panel shows the presence of hemispheric asymmetry in the presence of the HWM wind, although the simulation was conducted near the spring equinox. The recovery of the hemispheric symmetry by the removal of the HWM wind in the bottom panel demonstrates that the interhemispheric wind was responsible for the formation of hemispheric asymmetry. The two panels show the formation of an ionization trough at the magnetic equator and EIA crests near ±12° magnetic latitudes. In both cases, the longitudinal difference in the plasma density is not pronounced at the three longitude regions. The development of a slightly stronger EIA at 155° E is attributed to the larger upward velocity before noon at this longitude (see Fig. 2).

For the comparison of the SF $\boldsymbol{E}\times\boldsymbol{B}$ drift model with the ROCSAT-1 observations, we produced the vertical drift patterns at 45° E, 95° E, and 155° E using the ROCSAT-1 data during equinox in 1999–2002 under the condition $K_p \leq 3^+$. The mean vertical $\boldsymbol{E}\times\boldsymbol{B}$ drift velocity at the magnetic equator was calculated using data within ±5° magnetic latitudes at each 10° longitude bin. Figure 4 shows the ROCSAT-1 vertical $\boldsymbol{E}\times\boldsymbol{B}$ drifts at the three longitude sectors. The vertical bars on the plot at 95° E are the standard deviations.

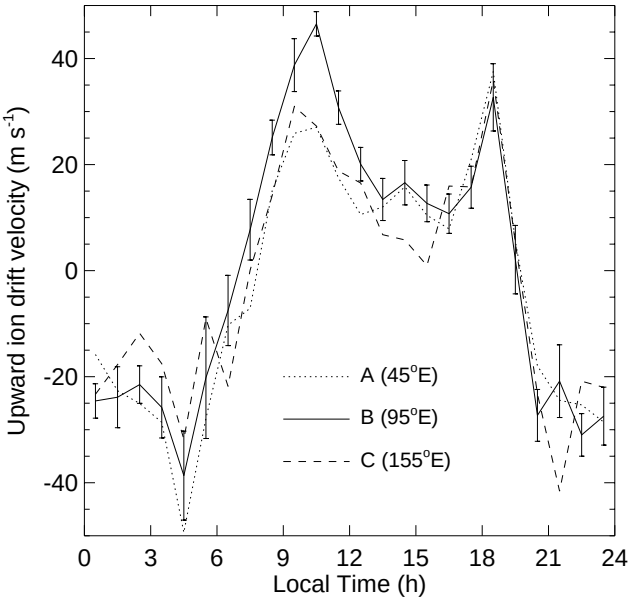

Fig. 4. The mean vertical $\boldsymbol{E}\times\boldsymbol{B}$ drift patterns at the three longitudes obtained from ROCSAT-1. The mean velocity at each local time was calculated using data within ±5° magnetic latitudes during equinox in 1999–2002.

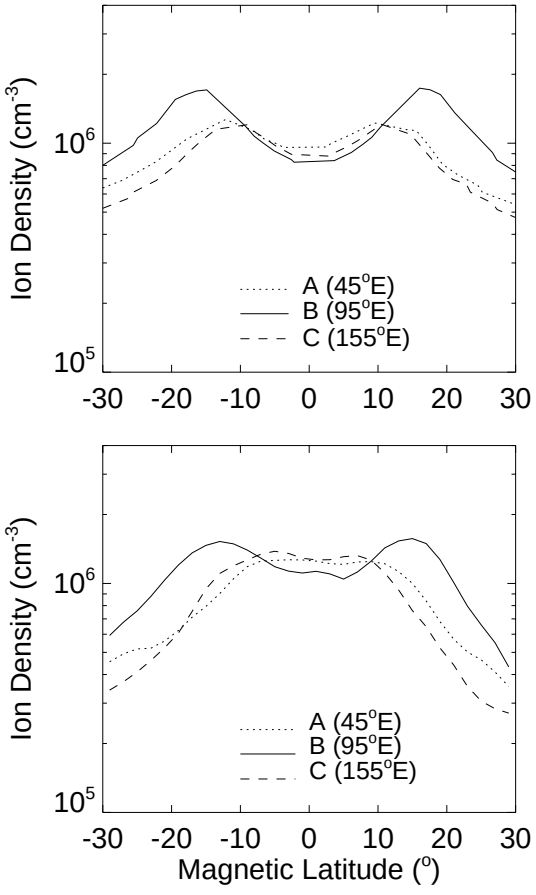

Fig. 5. The SAMI2 model plasma density profiles at an altitude of 600 km at 12:00–14:00 LT on 26 March 2002 calculated using the ROCSAT-1 drift data shown in Fig. 4 (top). The bottom panel shows the ROCSAT-1 density profiles at the three locations obtained from Fig. 1.

The formation of the longitudinally periodic plasma density structure is associated with the daytime upward $\boldsymbol{E}\times\boldsymbol{B}$ drift (Kil et al., 2008) and our main interest is the longitudinal difference of the vertical drift during daytime. The upward velocity at 95° E before noon is more pronounced than those at 45° E and 155° E. Compared with the SF $\boldsymbol{E}\times\boldsymbol{B}$ drift model, the ROCSAT-1 upward velocity is about 10–20 m s^{-1} greater than the SF model during 09:00–12:00 LT.

We conducted the SAMI2 model simulations after replacing the SF $\boldsymbol{E}\times\boldsymbol{B}$ drift model with the ROCSAT-1 drift patterns shown in Fig. 4. We are interested in the effect of the vertical $\boldsymbol{E}\times\boldsymbol{B}$ drift and the model simulations were conducted after the removal of the HWM wind. The top panel in Fig. 5 shows the mean model density profiles at 12:00–14:00 LT at an altitude of 600 km. The density profile at 95° E shows the development of a more pronounced EIA and a deeper equatorial ionization trough compared to those at the other two longitudes. For the comparison of the model ionosphere with the ROCSAT-1 observation, the bottom panel shows the ROCSAT-1 density profiles at the three longitudes. The longitudinal difference of the model ionosphere is consistent with the ROCSAT-1 observation. The model ionosphere shows the development of a stronger EIA and a deeper equatorial ionization trough compared with those in the ROCSAT-1 observation.

To test the capability to reproduce the observed wave-4 density structure by the effect of the vertical $\boldsymbol{E}\times\boldsymbol{B}$ drift, we conducted the SAMI2 model simulations at the 36 longitude sectors using the ROCSAT-1 drift data. The vertical ROCSAT-1 drift pattern at each 10° longitude bin was calculated using the data within ±5° magnetic latitudes during equinox in 1999–2002. Figure 6 presents the ROCSAT-1 density map (top), the SAMI2 model ionosphere obtained using the ROCSAT-1 drift data (middle), and the SAMI2 model ionosphere obtained using the SF $\boldsymbol{E}\times\boldsymbol{B}$ drift model (bottom). The model simulations were conducted under the conditions on 26 March 2002 after the removal of the HWM wind. The model ionosphere shows the mean density at 12:00–14:00 LT at an altitude of 600 km. The mean vertical drift velocities at 12:00–14:00 LT obtained from ROCSAT-1 and SF $\boldsymbol{E}\times\boldsymbol{B}$ drift model are also shown in the middle and bottom panels, respectively. The formation of the wave-4 structure is clearly seen in the middle panel. The longitudes of the crests and troughs of the wave-4 structure in the model ionosphere in the middle panel coincide with the longitudes of the crests and troughs in the ROCSAT-1 density and vertical drift data. The longitudinal variation of the SF model $\boldsymbol{E}\times\boldsymbol{B}$ drift is small and the model ionosphere produced using

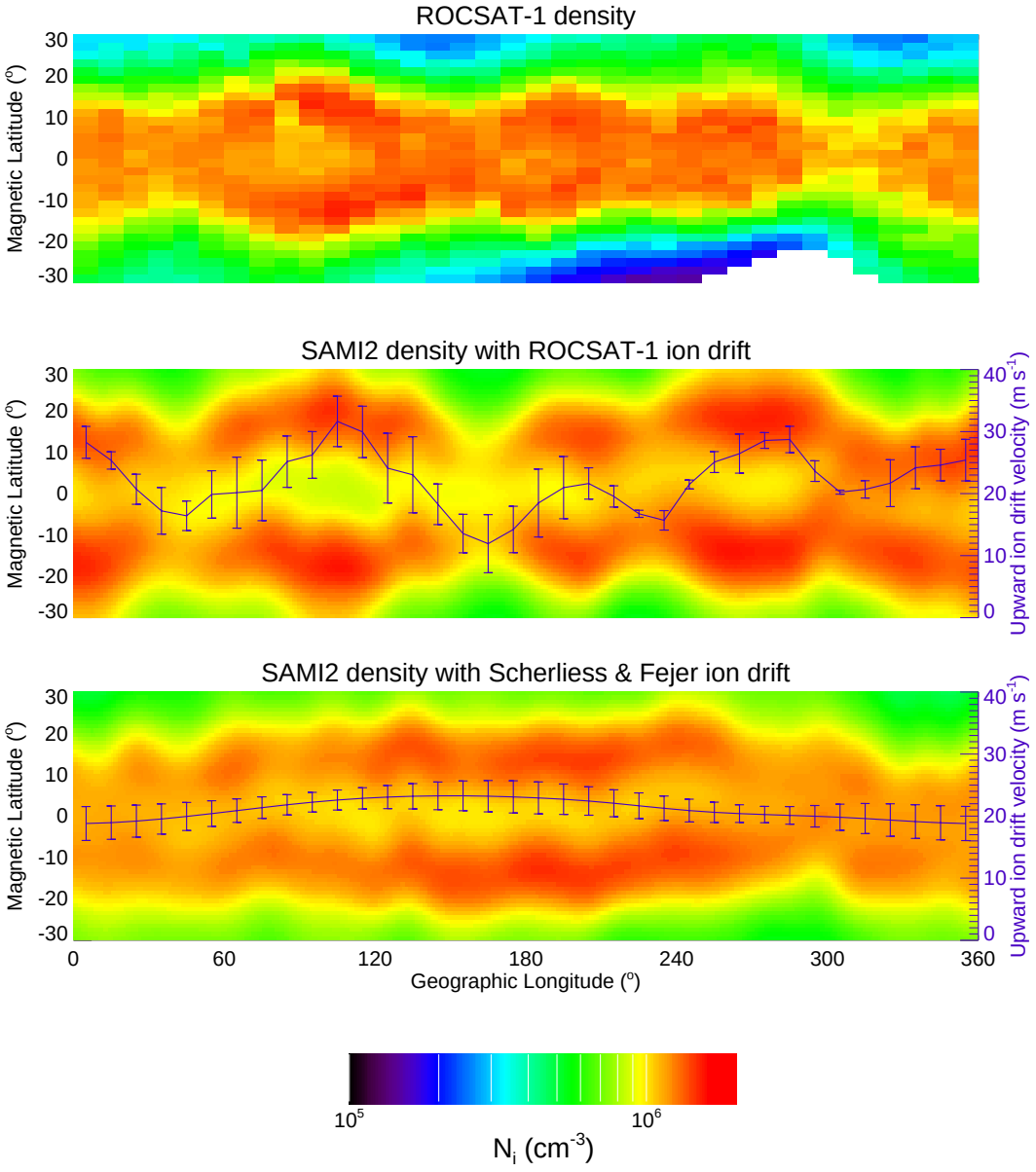

Fig. 6. Comparison of the longitudinal density structures at 12:00–14:00 LT during equinox obtained from ROCSAT-1 (top) with SAMI2 model ionosphere (middle and bottom). The top panel is the same as Fig. 1. The middle panel shows the SAMI2 model density map obtained using the ROCSAT-1 drift data. The blue curve shows the mean vertical ion velocity at 12:00–14:00 LT observed from ROCSAT-1. The vertical bars show the standard deviations. The bottom panel shows the SAMI2 model density map obtained using the SF $\boldsymbol{E}\times\boldsymbol{B}$ drift model. The blue curve shows the mean vertical ion velocity at 12:00–14:00 LT obtained from the SF $\boldsymbol{E}\times\boldsymbol{B}$ drift model. The SAMI2 model simulations were conducted on 26 March 2002.

the SF drift model does not show the formation of the wave-4 density structure.

The SAMI2 model simulations verified that the longitudinal variation of the vertical plasma drift observed by ROCSAT-1 is significant enough to produce the observed wave-4 density structure. While the peak longitudes of the model density structure coincided with the peak longitudes of the observed density structure, there existed some notable differences in the amplitudes of the density peaks between the model ionosphere and the ROCSAT-1 observation. The model ionosphere produced a deeper ionization trough at the magnetic equator and a wider separation of the northern and southern EIAs compared to the ROCSAT-1 observation. The model ionosphere produced using the SF $\boldsymbol{E}\times\boldsymbol{B}$ drift model also showed the development of the deeper ionization trough at the magnetic equator. The amplitude of a density crest near 270° E was much weaker than that near 100° E on the ROCSAT-1 data. On the other hand, the amplitude of the EIA

near 270° E was comparable to that near 100° E in the model ionosphere produced using the ROCSAT-1 drift data. Those discrepancies may arise from the possible errors in the input $\boldsymbol{E}\times\boldsymbol{B}$ drift and the uncertainties in the SAMI2 model. The zonal wind and neutral composition are important factors for the formation of the ionospheric morphology. The amplitudes of the wave-4 density structure produced by the effect of the vertical $\boldsymbol{E}\times\boldsymbol{B}$ drift can be modified by the longitudinal variation of those factors. The formation of deeper equatorial ionization trough in the model ionosphere may indicate that the equatorial plasma diffusion along the magnetic field lines occurs faster than the reality in the SAMI2 model. At this point, we cannot determine to what extent the discrepancies between the model ionosphere and observation were induced by the errors in the input $\boldsymbol{E}\times\boldsymbol{B}$ drift or by the uncertainties in the SAMI2 model. Further model simulations using different models are necessary to clarify the ionospheric response to the vertical $\boldsymbol{E}\times\boldsymbol{B}$ drift.

5 Development of a new vertical $\boldsymbol{E}\times\boldsymbol{B}$ drift model in the future

The SF $\boldsymbol{E}\times\boldsymbol{B}$ drift model has been widely used as a representative model of the vertical plasma drift in the equatorial ionosphere. The longitudinal mean vertical drift pattern is similar to the observation at Jicamarca but the longitudinal structure of the SF $\boldsymbol{E}\times\boldsymbol{B}$ drift model is significantly different from the observed longitudinal structures of the equatorial electrojet and vertical drift on the topside. There are some reasons why the SF $\boldsymbol{E}\times\boldsymbol{B}$ drift model is not able to represent the longitudinal structure of the vertical $\boldsymbol{E}\times\boldsymbol{B}$ drift. First, the AE-E data did not provide sufficient temporal and spatial coverage for the development of longitudinally high resolution $\boldsymbol{E}\times\boldsymbol{B}$ drift model. Second, the grouping of the longitude sectors following the magnetic field configuration was not an effective method. The longitudinal $\boldsymbol{E}\times\boldsymbol{B}$ drift structure inferred from the observations of equatorial electrojet (England et al., 2006a) and in situ ion velocity measurements (Kil et al., 2007) did not show any notable dependence on the geomagnetic field configuration. Third, the combination of the AE-E data with Jicamarca radar data in the Peruvian sector might rather increase errors in that sector since the $\boldsymbol{E}\times\boldsymbol{B}$ drift is largely variable in the Peruvian sector. The observations of the equatorial electrojet and $\boldsymbol{E}\times\boldsymbol{B}$ drift velocity showed the occurrence of their crests near 270° E and trough near 300° E. Weighting of the AE-E data with the Jicamarca data may smooth out the actual variation of the $\boldsymbol{E}\times\boldsymbol{B}$ drift in the Peruvian sector.

Currently, ROCSAT-1 provides a unique database for the development of a new vertical $\boldsymbol{E}\times\boldsymbol{B}$ drift model in the equatorial region. The number of total equator crossings (ascending and descending) of ROCSAT-1 during 5.5 years is about 58 000. If we bin the drift data with $24\times12\times36$ local time, month, and longitude grids, the number of data in each bin falls to 5∼6. Further division of the data with solar flux and magnetic activity will reduce the number of the data points to only a few. The reason that we produced the mean drift patterns in equinox using the ROCSAT-1 data of a few years was to acquire a sufficient number of data points for each local time and longitude bin. The number of data points can be improved by increasing the bin size. For example, we can group a few months into one bin if the variation of the $\boldsymbol{E}\times\boldsymbol{B}$ drift is small during those months. The bin size of the local time and longitude can also be adjusted depending on the variability of the vertical velocity with those parameters. The major reason that we do not have a sufficient number of data points is because we confined the use of data to near the magnetic equator. If the latitudinal variations of the vertical drift data can be properly modeled, we can develop a temporally and spatially higher resolution vertical $\boldsymbol{E}\times\boldsymbol{B}$ drift model using the ROCSAT-1 data. The solar flux is known to be an important parameter in determining the magnitude of the vertical plasma drift (Fejer et al., 1999). If the solar flux dependence of the vertical drift is significant only near the terminator, for example, we may use the solar flux criterion only during the limited local time period. The solar flux is dependent on the solar cycle but it is not yet clear which factor is more important for the variations of the vertical plasma drift. The solar cycle may be a more useful parameter than the solar flux if the response of the E-region dynamo electric field to the change of the solar flux occurs slowly. The dependence of the vertical plasma drifts on the solar flux and solar cycle is itself an interesting research subject. We can identify the solar cycle dependence only during the half solar cycle (5.5 years) near the solar maximum period using the ROCSAT-1 data. It will be possible to investigate the dependence of the vertical drift on the 27-day solar rotation period if we can extend the use of ROCSAT-1 data to higher latitudes. The dependence of the vertical drift on the 27-day solar rotation may indicate that the response of the dynamo electric field to solar flux is prompt. In the future, we will investigate the variability of the ROCSAT-1 vertical drift data for various factors and develop a new vertical $\boldsymbol{E}\times\boldsymbol{B}$ drift model.

6 Conclusions

The role of the vertical plasma drift for the formation of the longitudinally periodic plasma density structure in the low-latitude F region was investigated by conducting SAMI2 model simulations. The SAMI2 model simulations were conducted during equinox in 2002 using two different vertical $\boldsymbol{E}\times\boldsymbol{B}$ drift models. The model ionosphere produced using the ROCSAT-1 $\boldsymbol{E}\times\boldsymbol{B}$ drift data showed the development of wave-4 density structure that is similar to the density structure observed by ROCSAT-1. On the other hand, the model ionosphere produced using the SF $\boldsymbol{E}\times\boldsymbol{B}$ drift model could not reproduce the observed longitudinal density structure. The low-latitude ionosphere cannot be properly modeled

without using realistic vertical $\boldsymbol{E}\times\boldsymbol{B}$ drift. Our model simulation results demonstrated the capability to model the low-latitude ionosphere using the ROCSAT-1 drift data. In the near future, we will further refine the ROCSAT-1 drift data and develop a new vertical $\boldsymbol{E}\times\boldsymbol{B}$ drift model that may replace the current empirical $\boldsymbol{E}\times\boldsymbol{B}$ drift model.

Acknowledgements. H. Kil acknowledges support from NASA grant NNX08AF32G. W.-T. Kim was supported by KICOS through grant K20702020016-07E0200-01610 provided by MOST. Y.-H. Kim acknowledge the support from KOSEF grant funded by MOST (No. RO1-2006-0000-11003-0). The authors thank S.-Y. Su for providing the ROCSAT-1 data.

Topical Editor M. Pinnock thanks C. Vineeth and J. D. Huba for their help in evaluating this paper.

References

England, S. L., Maus, S., Immel, T. J., and Mende, S. B.: Longitudinal variation of the E-region electric fields caused by atmospheric tides, Geophys. Res. Lett., 33, L21105, doi:10.1029/2006GL027465, 2006a.

England, S. L., Immel, T. J., Sagawa, E., Henderson, S. B., Hagan, M. E., Mende, S. B., Frey, H. U., Swenson, C. M., and Paxton, L. J.: Effect of atmospheric tides on the morphology of the quiet time, postsunset equatorial ionospheric anomaly, J. Geophys. Res., 111, A10S19, doi:10.1029/2006JA011795, 2006b.

Fejer, B. G., Scherliess, L., and de Paula, E. R.: Effects of the vertical plasma drift velocity on the generation and evolution of equatorial spread F, J. Geophys. Res., 104, 19 859–19 869, 1999.

Hagan, M. E., Maute, A., Roble, R. G., Richmond, A. D., Immel, T. J., and England, S. L.: Connections between deep tropical clouds and the Earth's ionosphere, Geophys. Res. Lett., 34, L20109, doi:10.1029/2007GL030142, 2007.

Hartman, W. A. and Heelis, R. A.: Longitudinal variations in the equatorial vertical drift in the topside ionosphere, J. Geophys. Res., 112, A03305, doi:10.1029/2006JA011773, 2007.

Hedin, A. E.: Extension of the MSIS Thermospheric Model into the Middle and Lower Atmosphere, J. Geophys. Res., 96, 1159–1172, 1991.

Hedin, A. E., Biondi, M. A., Burnside, R. G., Hernandez, G., Johnson, R. M., Killeen, T. L., Mazaudier, C., Meriwether, J. W., Salah, J. E., Sica, R. J., Smith, R. W., Spencer, N. W., Wickwar, V. B., and Virdi, T. S.: Revised Global Model of Thermosphere Winds Using Satellite and Ground-Based Observations, J. Geophys. Res., 96, 7657–7688, 1991.

Huba, J. D., Joyce, G., and Fedder, J. A.: Sami2 is another model of the ionosphere (SAMI2): A new low-latitude ionosphere model, J. Geophys. Res., 105, 23 035–23 053, 2000.

Immel, T. J., Sagawa, E., England, S. L., Henderson, S. B., Hagan, M. E., Mende, S. B., Frey, H. U., Swenson, C. M., and Paxton, L. J.: Control of equatorial ionospheric morphology by atmospheric tides, Geophys. Res. Lett., 33, L15108, doi:10.1029/2006GL026161, 2006.

Kelley, M. C.: The Earth's Ionosphere, Academic Press, San Diego, California, 1989.

Kil, H., Oh, S.-J., Paxton, L. J., Zhang, Y., Su, S.-Y., and Min, K.-W.: Spike-like change of the vertical $\boldsymbol{E}\times\boldsymbol{B}$ drift in the equatorial region during very large geomagnetic storms, Geophys. Res. Lett., 34, L09103, doi:10.1029/2007GL029277, 2007.

Kil, H., Talaat, E. R., Oh, S.-J., Paxton, L. J., England, S. L., and Su, S.-Y.: The wave structures of the plasma density and vertical $\boldsymbol{E}\times\boldsymbol{B}$ drift in low-latitude F region, J. Geophys. Res., accepted, 2008.

Lin, C. H., Wang, W., Hagan, M. E., Hsiao, C. C., Immel, T. J., Hsu, M. L., Liu, J. Y., Paxton, L. J., Fang, T. W., and Liu, C. H.: Plausible effect of atmospheric tides on the equatorial ionosphere observed by the FORMOSAT-3/COSMIC: Three-dimensional electron density structures, Geophys. Res. Lett., 34, L11112, doi:10.1029/2007GL029265, 2007.

Lühr, H., Haüsler, K., and Stolle, C.: Longitudinal variation of F region electron density and thermospheric zonal wind caused by atmospheric tides, Geophys. Res. Lett., 34, L16102, doi:10.1029/2007GL030639, 2007.

Mouël, J.-L., Shebalin, P., and Chulliat, A.: The field of the equatorial electrojet from CHAMP data, Ann. Geophys., 24, 415–527, 2006,
http://www.ann-geophys.net/24/415/2006/.

Sagawa, E., Immel, T. J., Frey, H. U., and Mende, S. B.: Longitudinal structure of the equatorial anomaly in the nighttime ionosphere observed by IMAGE/FUV, J. Geophys. Res., 110, A11302, doi:10.1029/2004JA010848, 2005.

Scherliess, L. and Fejer, B. G.: Radar and satellite global equatorial *F*-region vertical drift model, J. Geophys. Res., 104(A4), 6829–6842, 1999.

Scherliess, L., Thompson, D. C., and Schunk, R. W.: Longitudinal variability of low-latitude total electron content: Tidal influences, J. Geophys. Res., 113, A01311, doi:10.1029/2007JA012480, 2008.

Su, S.-Y., Yeh, H. C., Heelis, R. A., Wu, J. M., Yang, S. C., Lee, L. F., and Chen, H. L.: The ROCSAT-1 IPEI preliminary results: Low-latitude ionospheric plasma and flow variations, Terr. Atmos. Oceanic Sci., 10, 787–804, 1999.